

Preserving entanglement and nonlocality in solid-state qubits by dynamical decoupling

R. Lo Franco,^{1,2,3,*} A. D'Arrigo,^{4,5} G. Falci,^{4,5,6} G. Compagno,¹ and E. Paladino^{4,5,6}

¹*Dipartimento di Fisica e Chimica, Università degli Studi di Palermo, Via Archirafi 36, 90123 Palermo, Italy*

²*Instituto de Física de São Carlos, Universidade de São Paulo,
Caixa Postal 369, 13560-970 São Carlos, São Paulo, Brazil*

³*School of Mathematical Sciences, The University of Nottingham,
University Park, Nottingham NG7 2RD, United Kingdom*

⁴*Dipartimento di Fisica e Astronomia, Università di Catania, Via Santa Sofia 64, 95123 Catania, Italy*

⁵*CNR-IMM UOS Catania (Università), Consiglio Nazionale delle Ricerche, Via Santa Sofia 64, 95123 Catania, Italy*

⁶*Istituto Nazionale di Fisica Nucleare, Sezione di Catania, Via Santa Sofia 64, 95123 Catania, Italy*

(Dated: September 1, 2014)

In this paper we study how to preserve entanglement and nonlocality under dephasing produced by classical noise with large low-frequency components, as $1/f$ noise, by Dynamical Decoupling techniques. We first show that quantifiers of entanglement and nonlocality satisfy a closed relation valid for two independent qubits locally coupled to a generic environment under pure dephasing and starting from a general class of initial states. This result allows to assess the efficiency of pulse-based dynamical decoupling for protecting nonlocal quantum correlations between two qubits subject to pure-dephasing local random telegraph and $1/f$ -noise. We investigate the efficiency of an “entanglement memory” element under two-pulse echo and under sequences of periodic, Carr-Purcell and Uhrig dynamical decoupling. The Carr-Purcell sequence is shown to outperform the other sequences in preserving entanglement against both random telegraph and $1/f$ noise. For typical $1/f$ flux-noise figures in superconducting nanocircuits, we show that entanglement and its nonlocal features can be efficiently stored up to times one order of magnitude longer than natural entanglement disappearance times employing pulse timings of current experimental reach.

PACS numbers: 03.67.Pp, 03.65.Ud, 07.05.Dz

I. INTRODUCTION

Controlling the dynamics of entanglement and preventing its disappearance due to decoherence¹ and via peculiar phenomena as the entanglement sudden death (ESD)², is a key requisite for any implementation of quantum information processing. For instance an entanglement memory element based on solid-state qubits will be strongly affected by dephasing due to noise sources with typical $1/f$ power spectrum³. To circumvent this problem it has been proposed to use hybrid systems combining superconducting nanocircuits with microscopic systems (atoms or defects), these latter having much longer coherence times and being suited to store quantum information^{4,5}. Actually networking with different platforms has a much wider scenario of potential applications, and it is believed to be the pathway towards the implementation of quantum hardware, despite of the obvious advantages (fabrication, control and scalability) of performing both quantum operations and storage on a single platform. Such applications, and other technologies as security-proof quantum key distribution and quantum communication complexity⁶⁻⁹, depend critically on the existence of quantum correlations *and* nonlocality, witnessing non-classically-reproducible entanglement^{10,11}.

In this paper we address the relevant and still unsolved question of how to preserve *entanglement and nonlocality* under dephasing produced by classical noise with large low-frequency components, as $1/f$ noise. To this end we investigate protection by dynamical decoupling (DD)

techniques^{3,12} focusing on an “entanglement memory”, physically implemented by a bipartite solid state nanodevice. The physical message of our work is that DD operated by control resources within the present technologies allows to preserve quantum correlations for times long enough to perform two-qubit quantum operations.

Originally developed in nuclear magnetic resonance¹³ DD techniques find important applications to quantum hardware¹⁴. They are open-loop (feedback-free) control methods for Hamiltonian engineering, thereby they do not require additional resources as encoding overheads or measurements capabilities. The strategy is dynamical averaging of environmental noise by suitably tailored pulse sequences¹². The prototype is spin-echo¹⁵, employing a single π pulse to cancel unwanted static couplings in the Hamiltonian, since the effect of the environment accumulated before the pulse is canceled during the subsequent “reversed” evolution. The Periodic DD (PDD), consisting in a train of such pulses separated by Δt , attenuates the effects of noise^{12,16} especially at low frequencies, $\omega \lesssim 1/\Delta t < 1/\tau_c$, where τ_c is the correlation time of the environment. In this work we consider PDD along with improved versions of DD sequences, namely the Carr-Purcell (CP)¹⁷ and the Uhrig DD (UDD)^{18,19} sequences. Pulse timing in these latter protocols is arranged in a way to produce higher order cancellations²⁰ in the Magnus expansion of the system “average Hamiltonian”¹³, yielding a stronger protection from noise.

It is known that DD techniques efficiently fight decoherence¹² affecting single qubits, especially in the relevant case of the $1/f$ environment³. Indeed it has been

shown that PDD achieves substantial decoupling, mitigating dephasing due to random telegraph noise (RTN) and to $1/f$ noise, both for quantum^{21–23} and for classical^{24–28} models. More recently the performances of optimized sequences have been analyzed^{20,29,30}. Routinely in experiments with superconducting qubits spin- or Hahn-echo^{31–34} are seen to reduce defocusing due to noise sources of various origin with $1/f^\alpha$ spectrum. Recently control by PDD, CP, CP-Meiboom-Gill and UDD sequences has been successfully implemented^{35–37}.

The possibility to preserve entanglement via various DD sequences has been also theoretically investigated recently^{38–41} for finite-dimensional or harmonic quantum environments. Concerning $1/f$ noise, enhancement of the lifetime of an entangled state of a superconducting flux qubit coupled to a microscopic two-level fluctuator⁴² has been observed under DD sequences. Experimental demonstrations of DD protection of bipartite entanglement from a solid-state environment have also been reported^{43–46} for ensembles of nuclear, impurity and electron spin-1/2.

The results we present in this paper show that DD sequences are able to preserve entanglement, ensuring at the same time the existence of nonlocality, for a wide class of mixed initial states in a pure dephasing environment. To this end we prove a relation between entanglement quantified by the concurrence⁴⁷, and nonlocality identified by the violation of a Bell inequality¹⁰. For realistic figures of $1/f$ noise^{35,42} protection for times more than one order of magnitude longer than ESD times is achieved, allowing advanced applications based on nonlocality. Notice that in our proposal DD fighting $1/f$ noise is implemented avoiding non-local control, and using pulse rates well within present experimental capabilities^{35,42}.

The paper is organized as follows. In Section II we derive the relation between entanglement and nonlocality for extended Werner-like (EWL) under a pure dephasing dynamics. In Section III we introduce the model and the DD sequences, illustrating then our approach to evaluate the concurrence. In Section IV we analyze the case study of RTN. We address the performance of DD sequences in the presence of local pure dephasing $1/f$ noise in Section V. Finally Section VI is devoted to the conclusions.

II. RELATION BETWEEN ENTANGLEMENT AND NONLOCALITY AT PURE DEPHASING

Strongly entangled systems are characterized by the presence of quantum correlations that cannot be reproduced by any classical local model. In these cases Quantum Mechanics exhibits nonlocality, which would guarantee resources for quantum technologies as secure quantum cryptography^{6,7,9}. For pure states entanglement always corresponds to the presence of nonlocality, but this is not the case in general. In fact mixed states exist whose correlations can be reproduced by a classical local model⁴⁸,

while they are entangled, as indicated by a nonzero value of the concurrence⁴⁷ $C(t)$. Nonlocality in such cases is unambiguously identified if Bell inequalities are violated. Therefore the Bell function \mathcal{B} , as defined by the Clauser-Horne-Shimony-Holt (CHSH) form¹⁰, can be used to seek whether the system exhibits nonlocal correlations, which occurs with certainty if $\mathcal{B} > 2$.

The possible existence of closed relations between quantifiers of entanglement and nonlocality is currently an open issue of special interest in dynamical contexts^{49–51}. A relevant question is establishing, for a given time evolution, whether a threshold value of concurrence exists ensuring nonlocal quantum correlations. More generally, the presence of such correlations would guarantee resources for quantum technologies as secure quantum cryptography^{6,7,9}, thereby efficient DD sequences must preserve entanglement above this threshold.

In this Section we analyze the relation between quantifiers of entanglement and nonlocality for two noninteracting qubits, A and B , locally subject to a pure dephasing interaction with the environment. Each qubit has Hamiltonian ($\hbar = 1$, $s = A, B$)

$$H_s = -\frac{\Omega_s}{2}\sigma_z^s - \frac{\hat{X}^s}{2}\sigma_z^s + \hat{H}_R^s, \quad (1)$$

where Ω_s is the Bohr frequency of qubit- s and \hat{X}^s represents a collective environmental operator coupled to the same qubit. The free evolution of the environment is included in \hat{H}_R^s . The overall Hamiltonian is thus $H = H_A + H_B$. Results of the present Section are valid for any \hat{H}_R^s and \hat{X}^s .

We suppose the two qubits are prepared in an EWL state

$$\rho_1 = r|1_a\rangle\langle 1_a| + \frac{1-r}{4}\mathbb{1}_4, \quad \rho_2 = r|2_a\rangle\langle 2_a| + \frac{1-r}{4}\mathbb{1}_4, \quad (2)$$

where the pure parts $|1_a\rangle = a|01\rangle + b|10\rangle$ and $|2_a\rangle = a|00\rangle + b|11\rangle$ are, respectively, the one-excitation and two-excitation Bell-like states with $|a|^2 + |b|^2 = 1$. When $a = b = 1/\sqrt{2}$ the EWL states reduce to the Werner states, a subclass of Bell-diagonal states^{10,52}. The density matrix of EWL states, in the computational basis $\{|0\rangle \equiv |00\rangle, |1\rangle \equiv |01\rangle, |2\rangle \equiv |10\rangle, |3\rangle \equiv |11\rangle\}$, is non-vanishing only along the diagonal and anti-diagonal (X form). The purity $P = \text{Tr}(\rho^2)$ of EWL states only depends on the purity parameter r and it is given by $P = (1 + 3r^2)/4$. The initial entanglement is equal for both the EWL states of Eq. (2) with concurrence $C_{\rho_1}(0) = C_{\rho_2}(0) = 2\max\{0, (|ab| + 1/4)r - 1/4\}$. Initial states are thus entangled for $r > \bar{r} = (1 + 4|ab|)^{-1}$.

Since the two qubits are noninteracting, the evolution of entanglement and nonlocality can be simply obtained from the knowledge of single-qubit dynamics⁵³. Under a pure dephasing evolution, for each qubit the diagonal elements of the density matrix in the eigenstate basis remain unchanged. The single-qubit coherences evolve in time $q_s(t) \equiv \rho_{01}^s(t)/\rho_{01}^s(0)$, the explicit time dependence being specified by the environmental properties

and the interaction term. If the system is subject to pure dephasing only, the X form of the density matrix is kept at $t > 0$. In particular, diagonal elements remain constant whereas antidiagonal elements evolve in time. They are related to the single qubit coherences by $\rho_{12}(t) = \rho_{12}(0)q_A(t)q_B^*(t)$ for the initial state ρ_1 and $\rho_{03}(t) = \rho_{03}(0)q_A(t)q_B(t)$ for ρ_2 . The concurrences at time t for the two initial states of Eq. (2) are given by⁵⁴ $C_{\rho_1}(t) = 2\max\{0, |\rho_{12}(t)| - \sqrt{\rho_{00}(0)\rho_{33}(0)}\}$ and $C_{\rho_2}(t) = 2\max\{0, |\rho_{03}(t)| - \sqrt{\rho_{11}(0)\rho_{22}(0)}\}$. For the pure dephasing evolution, it easy to show that $C_{\rho_1}(t) = C_{\rho_2}(t) \equiv C(t)$ with

$$C(t) = 2\max\{0, r|a|\sqrt{1-|a|^2}|q_A(t)q_B(t)| - (1-r)/4\}. \quad (3)$$

We now turn to nonlocality. The maximum CHSH-Bell function \mathcal{B} for a general X state can be found in analytic form⁴⁸. It can be expressed as $\mathcal{B} = \max\{\mathcal{B}_1, \mathcal{B}_2\}$, where $\mathcal{B}_1, \mathcal{B}_2$ are functions of the density matrix elements^{49,55}. This quantity has been studied for independent qubits each coupled to a bosonic reservoir (cavity) with Markovian⁵⁶ and non-Markovian^{11,57} features. For independent qubits subject to local pure dephasing noise, the two functions $\mathcal{B}_1, \mathcal{B}_2$ have the same form for the initial EWL states of Eq. (2) and are given by

$$\begin{aligned} \mathcal{B}_1(t) &= 2\sqrt{r^2 + 4r^2|a|^2(1-|a|^2)|q_A(t)q_B(t)|^2}, \\ \mathcal{B}_2(t) &= 4\sqrt{2}r|a|\sqrt{1-|a|^2}|q_A(t)q_B(t)|. \end{aligned} \quad (4)$$

It is easily seen that $\mathcal{B}_1(t)$ is always larger than or equal to $\mathcal{B}_2(t)$, so that the maximum Bell function is $\mathcal{B}(t) = \mathcal{B}_1(t)$.

To find a closed relation between $\mathcal{B}(t)$ and $C(t)$ we first observe that, in order to achieve nonlocality, two-qubit entanglement is necessary, i.e. $C(t) > 0$. Under these conditions $C(t) = 2[r|a|\sqrt{1-|a|^2}|q_A(t)q_B(t)| - (1-r)/4]$ and from Eq. (4) we obtain

$$\mathcal{B}(t) = 2\sqrt{r^2 + 4[C(t)/2 + (1-r)/4]^2}. \quad (5)$$

We remark that this result is valid for *any* local pure-dephasing qubit-environment interaction, starting from an initial EWL state with a generic value of $a \neq 0, 1$. For example, when $r = 1$ (initial Bell-like state), Eq. (5) reduces to $\mathcal{B}(t) = 2\sqrt{1 + C(t)^2}$. This relation, known when the system is in a pure state⁵⁸ or in a Bell-diagonal state⁵², is here found to persist *during* the system evolution for more general states.

The threshold value for $C(t)$ ensuring that at time t it is $\mathcal{B}(t) > 2$ immediately derives from Eq. (5)

$$C_{\text{th}} = \sqrt{1 - r^2} - (1 - r)/2. \quad (6)$$

Thus, for initial EWL states evolving under any pure dephasing interaction, the system exhibits nonlocality at time t provided the concurrence $C(t)$ is larger than a threshold value C_{th} depending *only* on the system initial purity. The threshold is a decreasing function of the purity and for $r = 1$ it is $C_{\text{th}} = 0$.

This result has relevant implications in those quantum computing platforms allowing for accurate initial state preparation. In particular this is the case of superconducting nanodevices. Preparation of entangled states has been recently implemented in different laboratories^{59–67}. For instance, entangled states of two superconducting qubits with purity ≈ 0.87 and fidelity to ideal Bell states ≈ 0.90 have been experimentally generated by using a two-qubit interaction, mediated by a cavity bus in a circuit quantum electrodynamics architecture⁵⁹. These states may be approximately described as EWL states with $r = r_{\text{exp}} \approx 0.91$ and $|a| = 1/\sqrt{2}$, giving a value of initial concurrence $C = 0.865$ and a threshold value for having nonlocality with certainty $C_{\text{th}} \approx 0.37$. In the remainder of this paper, except when explicitly mentioned, we will use these parameters for the initial EWL state, and the threshold value $C_{\text{th}} \approx 0.37$ as a benchmark for entanglement protection.

III. MODEL AND DYNAMICAL DECOUPLING SEQUENCES

We consider a two-qubit entanglement memory element where each qubit is locally subject to an ensemble of classical bistable fluctuators at pure dephasing and to pulse-based DD as modeled by

$$H_s^{\text{DD}} = H_s + \mathcal{V}_s(t), \quad (7)$$

where single qubit Hamiltonian H_s is of the form of Eq. (1) and quantum control is operated by the external field included in $\mathcal{V}_s(t)$. The environmental operator \hat{X}_s is here replaced by the stochastic process $X_s(t) = \sum_i^N v_i \xi_i(t)$ where $\xi_i(t)$ is a bistable symmetric process randomly switching between 0 and 1 with an overall rate γ_i . The power spectrum of the equilibrium fluctuations of each $v_i \xi_i(t)$,

$$S_i(\omega) = \int_{-\infty}^{\infty} dt v_i^2 [\langle \xi_i(t)\xi_i(0) \rangle - \langle \xi_i(t)^2 \rangle] e^{i\omega t} \quad (8)$$

is a Lorentzian $S_i(\omega) = v_i^2 \gamma_i / [2(\gamma_i^2 + \omega^2)]$. Following the standard procedure^{3,68}, we model $1/f$ noise as due to an ensemble of N random telegraph processes, individual rates being distributed in the interval $\gamma_i \in [\gamma_m, \gamma_M]$ with probability density $\propto 1/\gamma$. This yields the power spectrum

$$S^{1/f}(\omega) \approx \frac{\pi \sigma^2}{\ln(\gamma_M/\gamma_m) \omega} \quad (9)$$

where the noise variance σ is related to the distribution of couplings v . Assuming a narrow distribution about the average \bar{v} we have $\sigma^2 = \bar{v}^2 N/4$ ⁶⁹.

For DD we consider sequences of an *even* number n of instantaneous π -pulses about the x -axis, orthogonal to the qubit-environment interaction. The pulses are applied at times $t_k = \delta_k t$, where t is the total evolution time

and $0 \leq \delta_k \leq 1$ with $k = 1, \dots, n$. In PDD $\delta_k = k/n$ and $\Delta t = t/n$, the last pulse being applied at the observation time t . A PDD sequence with $n = 2$ corresponds to the echo procedure. In the CP sequences $\delta_k = (k - 1/2)/n$, while in UDD $\delta_k = \sin^2[\pi k/(2n + 2)]$. In the limit of a two-pulse cycle, $n = 2$, UDD reduces to the CP sequence.

We suppose the qubits are prepared at time $t = 0$ in a EWL state by some interaction which is thereafter switched off. Since both noise and decoupling sequences act locally, the two-qubit density matrix is entirely expressed by the single qubit coherences $q_s(t)$. For the PDD we will rely on the exact analytic expression for a qubit affected by a *quantum* environment of bistable impurities^{21,70}. Here we specialize to the classical limit where each impurity produces RTN and compare with the Gaussian approximation where the coherence can be expressed as $q_s(t) = \exp\{-\Gamma_s(t)\}$ with²⁰

$$\Gamma_s(t) = \int_0^\infty d\omega S_s(\omega) \frac{f(\omega t)}{\pi \omega^2}, \quad (10)$$

where the “filter function” $f(\omega t)$ is specific to the pulse sequence¹⁸. For PDD it reads²⁸ $f_{\text{PDD}}(\omega t) = 2 \tan^2[\omega t/(2n)] \sin^2(\omega t/2)$. For the CP and UDD we will rely on the analysis of Ref.²⁸ where it has been found for single qubit coherence that down to a relatively small pulse rate the effect of RTN is reasonably approximated by a Gaussian (Ornstein-Uhlenbeck) process even under strong coupling conditions (see next Section for a quantitative definition). Therefore for CP and UDD we will resort to the Gaussian approximation Eq. (10) with filter functions (for an even number of pulses n) are $f_{\text{CP}}(\omega t) = 8 \sin^4[\omega t/(4n)] \sin^2(\omega t/2) / \cos^2[\omega t/(2n)]$ and $f_{\text{UDD}}(\omega t) = \frac{1}{2} |\sum_{k=-n-1}^n (-1)^k \exp[i\frac{\omega t}{2} \cos \frac{\pi k}{n+1}]|^2$ respectively. Equipped with these expressions for the single qubit coherences we can investigate time evolution of the entanglement by Eq. (3), using $q_s(t)$ as given by the specific expression for each sequence.

IV. DYNAMICAL DECOUPLING OF RANDOM TELEGRAPH NOISE

We now consider an entanglement memory element where each qubit is locally subject to RTN and to DD sequences. We first review the effect of RTN on evolution of the entanglement for the initial EWL states of Eq. (2) in the absence of pulses^{71,72}. This preliminary analysis puts the basis for the investigation of entanglement preservation by DD.

Entanglement under local RTN – The single qubit dynamics under these conditions has been investigated in several papers and here we briefly summarize the main findings. The qubit coherence for qubit $s = A, B$ is given by^{69,73}

$$q_s^{\text{RTN}}(t) = e^{-i\Omega_s t} [A_s e^{-\frac{\gamma_s(1-\alpha_s)t}{2}} + (1 - A_s) e^{-\frac{\gamma_s(1+\alpha_s)t}{2}}], \quad (11)$$

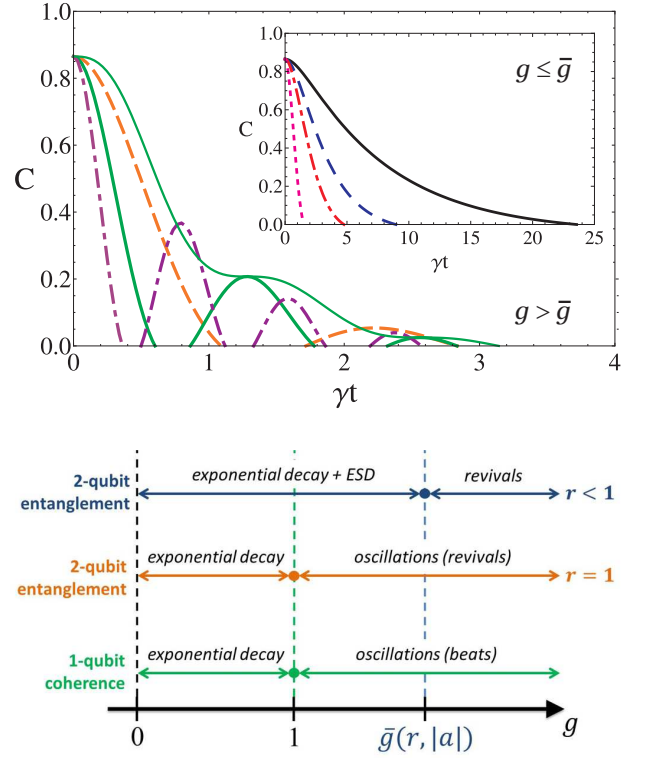


FIG. 1: (Color online) Top panel: Concurrence C as a function of γt under local RTNs with $g > \bar{g} \approx 2.3$ (EWL initial states with $r = 0.91$, $|a| = 1/\sqrt{2}$): $g = 3$ (dashed orange), $g = 5$ (thick green) and $g = 8$ (dot-dashed purple). We fixed $\delta p_0 = 0$ except for the thin green line which corresponds to $\delta p_0 = \pm 1$ for $g = 5$. In the inset $g < \bar{g}$: $g = 0.5$ (thick black), $g = 0.8$ (dashed blue), $g = 1.1$ (dot-dashed red) and $g = \bar{g} = 2.3$ (dotted magenta). Bottom panel: sketch of the threshold values of the dimensionless coupling parameter g separating dynamical regimes for single qubit and entanglement dynamics.

here $A_s = \frac{1}{2\alpha_s}(1 + \alpha_s - ig_s \delta p_{0,s})$ and $\alpha_s = \sqrt{1 - g_s^2}$ are expressed in terms of $g_s = v_s/\gamma_s$ and $\delta p_{0,s}$ is the initial population difference of the two states $\xi_s = 0, 1$. Repeated measurements with fully thermalized fluctuators are described by $\delta p_{0,s} = 0$, whereas other choices (e.g. $\delta p_{0,s} = \pm 1$) are appropriate for nonequilibrium conditions⁶⁹. For a weakly coupled fluctuator $g_s \ll 1$ the coherence decays exponentially with the rate $\Gamma = S_s(0) = v_s^2/(2\gamma_s)$, which is the standard golden rule result. Under these conditions the Gaussian approximation applies to the bistable process. In the strong coupling regime $g_s \geq 1$, the system exhibits damped beatings and, for $g_s \gg 1$ the decay rate saturates to γ_s . In this regime the non Gaussian nature of the stochastic process is clearly visible in the qubit evolution^{69,73}.

The concurrence of two uncoupled qubits each subject to a RTN process is readily found using Eq. (3) with $q_s(t)$ given by Eq. (11). For a pure initial entangled state, $r = 1$, $a \neq 0$, entanglement reflects the single-qubit coherence qualitative behavior. The concurrence either decays exponentially if $g_s < 1$ or displays damped beatings

	g							
	0.1	0.5	1.1	$\bar{g} = 2.3$	3	5	10	30
γt_{ESD}	600	23.60	4.75	1.50	1.09	0.6	0.28	0.09
γt_{FD}	600	23.60	4.75	1.50	2.83	2.83	2.68	2.76

TABLE I: Dimensionless ESD and FD times (scaled with γ) for different values of g for local RTNs and initial EWL states with $r = r_{\text{exp}} = 0.91$ and $|a| = 1/\sqrt{2}$. For $g > \bar{g}$, t_{ESD} has been identified as the first time at which entanglement disappears, $C(t_{\text{ESD}}) = 0$, thus $t_{\text{FD}} > t_{\text{ESD}}$.

if at least one g_s is larger than 1. The regime $r < 1$ instead reveals the new phenomenon of ESD, i.e. the concurrence² vanishes abruptly at a certain time t_{ESD} , and show qualitative different entanglement behavior for different values of the dimensionless couplings g_s . For identical qubit-RTN coupling conditions (i.e. for both $g_s = g$) a threshold value exists, separating a regime of exponential entanglement decay or ESD from a regime where entanglement revivals occur. This threshold value, not yet reported in the literature, only depends on the parametrization of the initial state and it is given by¹

$$\bar{g}(r, |a|) = \sqrt{1 + 4\pi^2 \left[\ln \left(\frac{4r|a|\sqrt{1-|a|^2}}{1-r} \right) \right]^{-2}}. \quad (12)$$

Since $r < 1$, it is $\bar{g} > 1$; for instance for $r = 0.91$ and $|a| = 1/\sqrt{2}$, we get $\bar{g} \approx 2.3$. When $g \leq \bar{g}$ the system displays ESD, whereas for $g > \bar{g}$ a “final death” (FD) of entanglement takes place, i. e. a definitive disappearance of entanglement after revivals. These behaviors are illustrated in the top panel of Fig. 1. The different dynamical regimes for single qubit and entanglement dynamics with respect to \bar{g} are schematically illustrated in the bottom panel of Fig. 1.

The ESD time for $g < 1$ can be simply derived from Eq. (11). When $g \ll 1$ and $\delta p_0 = 0$ the first term of Eq. (11) is much larger than the second one and, from Eq. (3), the ESD time (for equal $\gamma_s = \gamma$) is found as⁷²

$$t_{\text{ESD}}^{\text{RTN}} = -\frac{2/\gamma}{1 - \sqrt{1-g^2}} \ln \left(\frac{\sqrt{\frac{(1-g^2)(1-r)}{r|a|\sqrt{1-|a|^2}}}}{1 + \sqrt{1-g^2}} \right). \quad (13)$$

We checked numerically that the above expression provides a reasonable approximation up to $g = 0.9$. For larger values of g , the numerical ESD and FD times are reported in Table I. The dependence of the single-qubit coherence $q_s(t)$ on the initial population difference

$\delta p_{0,s}$ qualitatively affects the entanglement dynamics for $g > \bar{g}$, while it leaves it practically unchanged for $g \leq \bar{g}$ ⁷². In particular, when $g > \bar{g}$, the concurrence for $\delta p_0 = \pm 1$ does not exhibit revivals and it is always larger than for $\delta p_0 = 0$. The final death time is also longer than for $\delta p_0 = 0$ (see Fig. 1 for $g = 5$).

In the following, we shall see that the existence of a threshold value for g plays a role in the efficiency of the DD procedure to prevent complete entanglement disappearance under local RTNs. Hereafter the value of the initial population difference of RTN is set to the thermal equilibrium value $\delta p_0 = 0$.

A. Entanglement echo

For the two-pulse echo the qubit coherence reads^{21,73}

$$q_s^e(t) = \frac{e^{-\frac{\gamma_s t}{2}}}{\alpha_s^2} \left[\frac{1 + \alpha_s}{2} e^{\alpha_s \frac{\gamma_s t}{2}} + \frac{1 - \alpha_s}{2} e^{-\alpha_s \frac{\gamma_s t}{2}} - (1 - \alpha_s^2) \right], \quad (14)$$

where $t = 2\Delta t$. For the sake of simplicity, we assume that the two qubits are acted by simultaneous pulses applied at times Δt and $2\Delta t$. We consider two fluctuators with equal switching rates, $\gamma_s \equiv \gamma$, but differently coupled to the respective qubits $v_A \neq v_B$ in order to address different coupling regimes, $g_A \neq g_B$. The general outcome of this analysis is that the echo preserves entanglement with a qualitative behavior critically sensitive to the values of $\gamma\Delta t$ and g_s .

When the qubits experience the same coupling conditions, $g_s \equiv g$, the entanglement-echo efficiency reflects the presence of ESD or of FD in the unconditioned evolution, i.e. it depends on whether g is smaller or larger than \bar{g} . This behavior of “entanglement echo” is illustrated in Fig. 2(a). When $g \leq \bar{g}$ the ESD time is delayed, whereas for $g > \bar{g}$ the dynamical structure of entanglement revivals and dark periods is washed out by the echo procedure and entanglement exhibits plateau-like features. These latter reflect non-Gaussianity of the RT process, and are the counterpart of the plateaus of the single-qubit coherence in the strong coupling regime $g \gg 1$ ⁷³, observed in the experiment of Ref.³¹.

Plateaus occur also when $g_A \neq g_B$, provided at least one qubit is sufficiently strongly coupled, as shown in Fig. 2(b). The effect originates from echo pulses on the qubit affected by the strongly coupled fluctuator.

A figure of merit for the entanglement-echo efficiency is the concurrence at the echo time $t = 2\Delta t$. We analyze its behavior as a function of the couplings $g_s \equiv g$ in Fig. 3, and compare with the concurrence at the same times. As expected, for small pulse interval, $\Delta t \ll 1/\gamma$, echo is very effective in suppressing the noise, even for relatively large values of g . A richer scenario is found for $\Delta t \sim 1/\gamma$. In the absence of echo the concurrence at fixed $t = 2\Delta t$ is non-monotonic with g (see Fig. 3, thin solid line, for $t = 1/\gamma$). In particular in the limit $g \gg 1$, an analytic expression can be found the asymptotic ex-

¹ The expression of $\bar{g}(r, |a|)$ of Eq. (12) is obtained as follows. Firstly, one finds the time t_{max} corresponding to the first maximum of $C(t)$ of Eq. (3), assuming $g > 1$. Secondly, one looks for the values of g such that $C(t_{\text{max}}) > 0$, which in turn gives $g > \bar{g}(r, |a|)$.

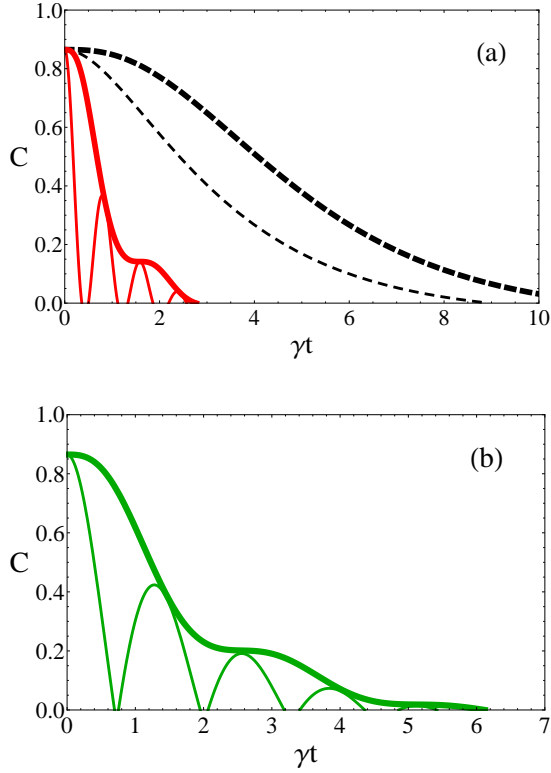


FIG. 2: (Color online) Concurrence $C(2\Delta t)$ at the end of the echo as a function of $\gamma t = 2\gamma\Delta t$, showing different "entanglement echo" behavior depending on $g \gtrless \bar{g} = 2.3$ (for the chosen initial state mentioned in the text). Panel (a): Cases $g_s = g = 0.8 < \bar{g}$ (dashed black lines) and $g = 8 > \bar{g}$ (solid red lines), with echo (thick lines) and without (thin lines). For $g = 8$ notice the plateau at $\gamma\Delta t = 2\pi/g \approx 0.8$. Panel (b): $g_A = 0.4$ and $g_B = 5$, with echo (thick line) and without (thin line).

pansion of Eq. (11), $|q_{\text{RTN}}(t)| \approx \exp(-\gamma t/2) \cos(g\gamma t/2)$. Such oscillations reflect the already discussed entanglement collapses and revivals as a function of time, occurring in the regime $g > \bar{g}$. Oscillatory behavior of C is observed also in the presence of the echo pulse (Fig. 3, thick solid lines). Interestingly, echo preserves entanglement even when it vanishes in the absence of the pulse. However, the recovered entanglement might still not be sufficient for efficient realization of quantum error correction tasks. Finally for increasing $\Delta t > 1/\gamma$, the echo procedure becomes more and more inefficient in reducing detrimental effects of noise, whatsoever g .

B. Entanglement protection by DD sequences

The above results suggest that a sequence of pulses may preserve entanglement for longer time. Here we investigate this issue for PDD, CP and UDD. For illustrative purposes it is sufficient to consider identical qubits, $g_s = g$.

We first study how entanglement-DD performs against RTN in both the strong and the weak coupling regimes,

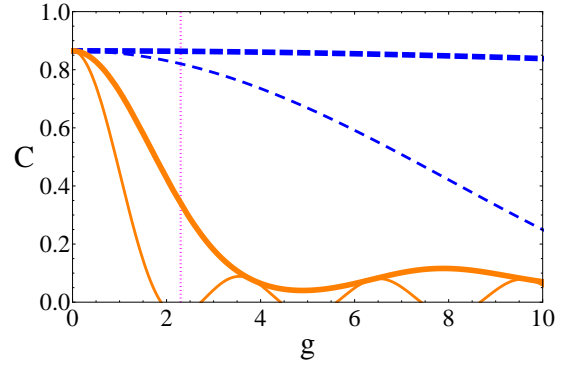


FIG. 3: (Color online) Concurrence after an echo sequence $C(2\Delta t)$, as a function of $g \equiv g_s$ (thick lines). It is shown the behavior for small pulse interval ($\gamma\Delta t = 0.1$ blue dashed line) and for larger interval ($\gamma\Delta t = 1$ orange solid line). For comparison the concurrence in the absence of echo at the same time $t = 2\Delta t$ is reported (thin dashed and solid lines).

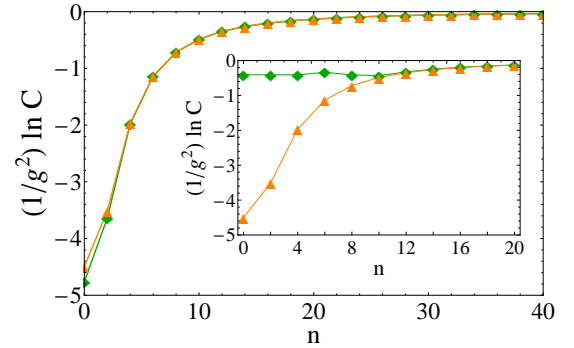


FIG. 4: (Color online) Comparison $[\ln C(\bar{t})]/g^2$, at the fixed time $\gamma\bar{t} = 10$ for PDD, as a function of the number of pulses n for RTN (green diamonds) and Gaussian (Ornstein-Uhlenbeck) noise (orange triangles). The values of g are 0.5 (principal panel) and 5 (inset). The initial state is pure maximally entangled.

for increasing pulse rate. We consider PDD sequences and evaluate the concurrence at fixed times \bar{t} and different number n of pulses equally spaced, $\Delta t = \bar{t}/n$. This quantity can be obtained from the exact result, Eq.(A1), on DD of a single qubit from a pure dephasing RT fluctuator^{21,70}. Moreover, in order to get insight on the effect of non-Gaussianity of RTN, we compare the above results, with their Gaussian approximation. In this latter the coherences are obtained using Eq.(10), where $S_s(\omega)$ is the power spectrum of an Ornstein-Uhlenbeck process.

In Fig. 4 we plot $[\ln C(\bar{t})]/g^2$ as a function of the (even) number of pulses n for $\gamma\bar{t} = 10$ and for an initial Bell state. Notice that in the Gaussian approximation¹², since $\Gamma_s(t) \propto g^2$, also the quantity $\ln[C(\bar{t})] = -[\Gamma_A(\bar{t}) + \Gamma_B(\bar{t})] \propto g^2$, thereby the combination plotted in Fig. 4 is universal. On the contrary a dependence on g related to non-Gaussianity appears for RTN. Actually for $g < 1$ (main panel) the exact result and the Gaussian

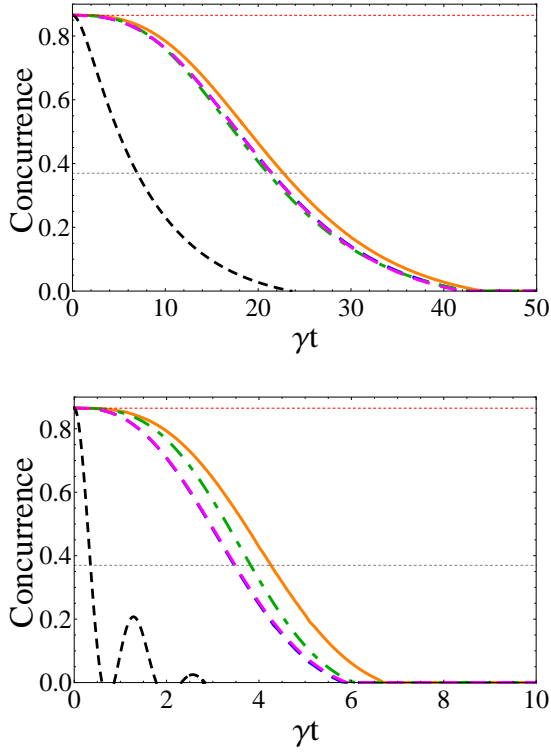


FIG. 5: (Color online) Concurrence as a function of the dimensionless time γt for $g = 0.5$ (top panel) and $g = 5$ (bottom panel) for a fixed number of pulses $n = 10$ ($\delta p_0 = 0$). Black dashed lines represent concurrences without DD sequences. Magenta long-dashed line, green dot-dashed line and orange solid line represent concurrences for PDD, UDD and CP, respectively. A blue long-dashed line is also displayed coinciding with the magenta one and representing PDD in Gaussian approximation. The gray dotted line at $C_{\text{th}} \approx 0.37$ represents threshold value of C for Bell inequality violation. The red dotted line at the top is the initial value of concurrence.

approximation practically coincide, showing that the discrete nature of RTN is not relevant in weak coupling, as expected on physical grounds even in the absence of pulsed control⁶⁹). Instead for $g > \bar{g}$ (inset) the equivalence is recovered only at large n , i.e. for sufficiently large pulse rates, where $\ln[C(\bar{t})]/g^2$ shows universal behavior. For intermediate rates $1/\Delta t \sim \gamma$, although PDD cancels dark periods and revivals (see Fig. 1), the entanglement recovered is relatively small since its decay is already relatively slow, $\sim e^{-2\gamma t}$.

The monotonic increase of $[\ln C(\bar{t})]/g^2$ with increasing pulse rate, $1/\Delta t$, shows how PDD suppresses the effect of RTN. In the universal regime $\gamma \Delta t \ll 1$, very frequent π -pulses about σ_x coherently average out the effect of RTNs with $\gamma \ll 1/\Delta t$ and partially reconstruct the initial entanglement, independently of the coupling regime. This argument holds more in general and explains why in this regime different statistical properties of Gaussian and non-Gaussian processes do not produce a distinguishable effect on the entanglement dynamics.

The above argumentation also suggests that the equiv-

alence at large pulse rates holds also for CP and UDD sequences in general. This can be shown explicitly by comparing the Gaussian approximations with entanglement calculated using the numerical solution for the qubit coherences in the presence of RTN²⁸. This analysis pointed out that high-order noise correlators in the decay factor of the qubit coherences are suppressed by CP and UDD, the former performing better than the latter, which is by construction optimized to reduce the second cumulant (Gaussian term). For the CP and UDD sequences the Gaussian approximation for the qubit coherences was found to be applicable up to $g = 10$ for $n = 10$ pulses²⁸.

Based on these considerations, in the following we study how entanglement is preserved as a function of time. We consider sequences with a fixed number n of pulses for each t . This would be the outcome of an experiment where the qubits evolve during runs of assigned duration t under the considered n -pulse sequence. The overall curve is recorded from successive runs varying t , but not n . We will use the Gaussian approximation for the coherences under the CP and UDD sequences, whereas for PDD we resort to the exact result form Eq.(A1).

Results, shown in Fig. 5 for $n = 10$ pulses illustrate that the DD procedures preserve entanglement at times longer than for its natural complete disappearance, independently on the coupling conditions. We notice that the different qualitative behaviors of the entanglement observed for $g \leq \bar{g}$ and $g > \bar{g}$ in the absence of pulses (see also Fig.(1)) are canceled by DD. Indeed, from the filter functions of the considered sequences it is easy to see that the application of n pulses within time t effectively suppresses the effect of noise components below frequency $\omega_n \sim 2n/t$ ²⁸. CP slightly outperforms UDD, PDD being the less effective sequence. Notice how effective are pulse sequences in the strong coupling regime (lower panel of Fig. 5): for instance, for $g = 5$, the CP sequence keeps the concurrence above the nonlocality threshold C_{th} for times ($\gamma t \approx 4.5$) an order of magnitude longer than in absence of pulses ($\gamma t \approx 0.4$). In the weak coupling regime DD extends to larger times the initial short times behavior. As a consequence nonlocality becomes more robust and the ESD times are delayed.

Another figure of merit of the DD sequences is how many pulses are required to store the entanglement until the ESD-FD times. To address this issue we evaluate the concurrence under DD at the time \bar{t} where it definitively vanishes under free evolution. These times depend on the coupling conditions and are given by the ESD times for $g \leq \bar{g}$ and by the FD times for $g > \bar{g}$ (see Table I). This analysis is reported in Fig. 6 for the CP sequence, that is the most efficient pulse sequence. Notice that the minimum number of pulses to store entanglement is obtained for $g = \bar{g} = 2.3$: already two pulses allow exceeding the threshold C_{th} , while ten pulses give $C = 0.857$. i.e. an error $\sim 0.9\%$ with respect to the initial value $C(0) = 0.865$. This is due to the fact that for $g = \bar{g}$ entanglement disappears completely in the shortest time (see table I). This means that small pulse intervals are

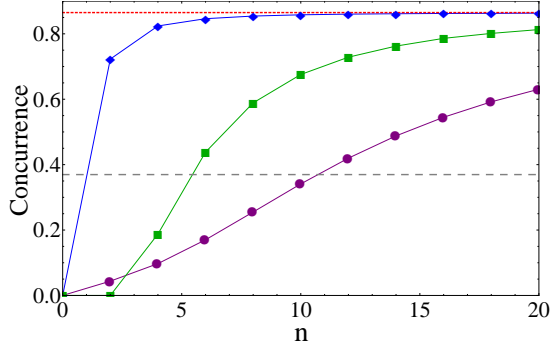


FIG. 6: (Color online) Concurrence under CP as a function of the number of pulses n at fixed times $\gamma\bar{t} = \gamma t_{\text{ESD}}$ for $g \leq \bar{g}$ and $\gamma\bar{t} = \gamma t_{\text{FD}}$ for $g > \bar{g}$. The values of g are 0.5 (purple circles), $\bar{g} = 2.3$ (blue diamonds) and 5 (green squares). The gray dashed line at $C_{\text{th}} \approx 0.37$ represents the threshold value of C after which there is a Bell inequality violation. The red dotted line is the initial value of concurrence.

needed, but on the other hand few of them very efficiently recover the large amount of entanglement initially lost in the absence of pulses, as shown by the fast initial increase of $C(\gamma\bar{t})$ in Fig. 6.

V. DYNAMICAL DECOUPLING OF $1/f$ NOISE

In this Section we investigate the efficiency of PDD, CP and UDD sequences to preserve entanglement between two superconducting qubits in the presence of pure-dephasing Broad Band Colored Noise (BBCN). This is the common instance in solid-state implementations of quantum processors. We refer to the experimental situation reported in Refs.^{35,36} where magnetic flux noise on a flux-type superconducting qubit has been well characterized. Consistent measurements of $1/f$ -type power laws have been reported at 0.2-20 MHz and in the range 0.01-100 Hz. Based on these results, we consider flux noise $S_{\Phi}(\omega) = A_{\Phi}/(2\pi\omega)$, extending between 1 Hz and 10 MHz with amplitude $A_{\Phi} = (1.7 \times 10^{-6} \Phi_0)^2$ ($\Phi_0 = h/(2e)$ is the magnetic flux quantum). For the above noise amplitude and $\gamma_i \in [1, 10^7]$ Hz, Eq.(9) yields $\sigma \approx 2\pi \times 10^7$ Hz. We attribute this figure of noise to a large number ($N = 10^4$) of impurities with a narrow distribution of couplings about the average $\bar{\nu}/2\pi = 0.2$ MHz. We remark that $\gamma_M = 10^7$ Hz is a soft UV-cut-off, the spectrum decaying as ω^{-2} at larger frequencies.

The single qubit coherence $q_{1/f}(t) = \prod_{i=1}^N q_i(t)$ is obtained as the product of N coherences $q_i(t)$ associated to each RTN, which in absence of pulses is given by Eq. (11). The resulting concurrence Eq. (3) allows to estimate the ESD-time which will be used as a benchmark for entanglement recovery. Using quasi-static $1/f$ -noise^{33,74} we have $t_{\text{ESD}} \approx 1/[\sigma \sqrt{\ln(4|ab|r/(1-r))}]^{75}$, and the corresponding figure for the initial EWL state and σ we consider is $t_{\text{ESD}} \approx 27$ ns.

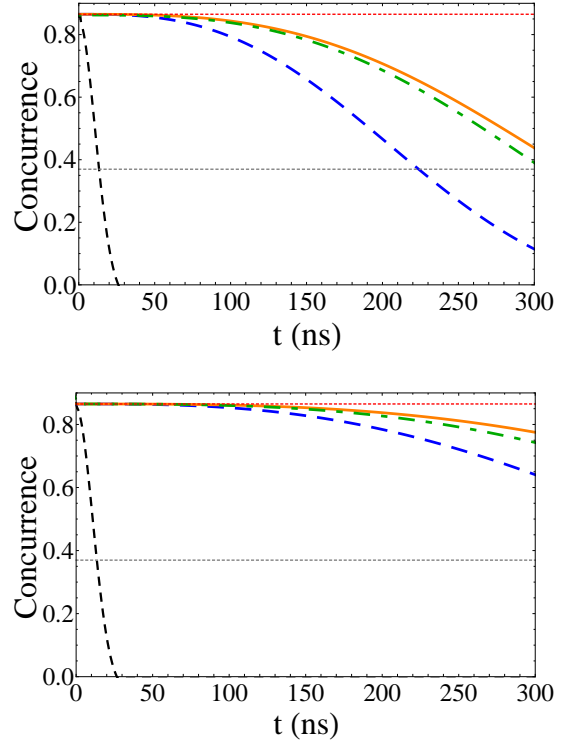


FIG. 7: (Color online) Concurrence as a function of time t at a fixed number of pulses $n = 4$ (top panel) and $n = 10$ (bottom panel). Blue long-dashed line, green dot-dashed line and orange solid line represent concurrences for PDD, UDD and CP, respectively. Black dashed line is the concurrence in absence of pulses, entanglement disappearing at $t_{\text{ESD}} \approx 27$ ns. The gray dotted line at $C_{\text{th}} \approx 0.37$ is the threshold value of C for after Bell inequality violation. The top red dotted line is the initial value of concurrence. The $1/f$ noise figures are given in the text.

Results for other sequences are found following the same steps. For PDD we use the exact $q_{\text{PDD}}(t)$ of Eq. (A1), whereas CP and UDD sequences are studied in the Gaussian approximation Eq. (10) for the qubit coherences, evaluated with $S^{1/f}(\omega)$ Eq.(9) and the appropriate filter functions. In each case we finally find the concurrences from Eq. (3).

The effectiveness of the considered DD sequences is analyzed in Fig. 7 where we display the concurrence vs time $t \in [0, 0.3 \mu\text{s}]$ for sequences with fixed number of pulses ($n = 4$ and $n = 10$). The CP sequence shows remarkable performances, since already 4 pulses allow to store entanglement for times $t \sim 500$ ns, much larger than $t_{\text{ESD}} \approx 27$ ns. For 10 CP pulses entanglement is preserved until $t \sim 900$ ns. It is worth stressing that the concurrence exceeds the non-locality threshold C_{th} for times scales relevant for computation, namely $t \sim 300$ ns with 4-pulses CP, to be compared with $t \approx 13$ ns in the absence of pulsed control. Operating 4 CP pulses in 300 ns is absolutely within current technologies³⁵ and there is room for improvement by higher pulse rates. We find that the CP sequence outperforms PDD and UDD, despite of the expectation that UDD gains from its strong low-

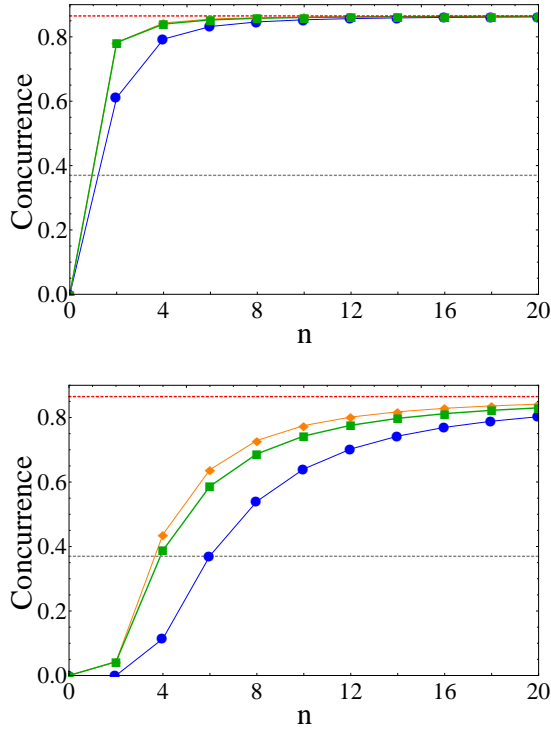


FIG. 8: (Color online) Concurrence as a function of the number of pulses n at $\bar{t}_1 = 0.1\mu\text{s}$ (top panel) and $\bar{t}_2 = 0.3\mu\text{s}$ (bottom panel). Blue circles, green squares and orange diamonds represent concurrences for PDD, UDD and CP, respectively. The CP points are superposed to the UDD ones. The gray dashed line at $C_{\text{th}} \approx 0.37$ represents the threshold value of C after which there is a Bell inequality violation. The red dotted line at the top is the initial value of concurrence.

frequency filtering properties. Therefore, CP sequence interestingly works best for entanglement protection in the no-cut-off case. This circumstance, which is also observed in experiments, is due in our model to the $\sim \omega^{-2}$ tail of the spectrum for frequencies larger than γ_M .

In Fig. 8 we study how increasing the number of pulses a high degree of entanglement and nonlocality at given times ($\bar{t}_1 = 0.1\mu\text{s}$ and $\bar{t}_2 = 0.3\mu\text{s}$), both much larger than t_{ESD} . Notice that we have short t_{ESD} since the problem addressed in this paper, namely $1/f$ noise at pure dephasing, is the “worse scenario” for dephasing. In a single qubit effects of noise with sharp UV-cut-off γ_M are strongly suppressed if $2n/\bar{t} > \gamma_M$, UDD yielding high-fidelity at short times and CP being more efficient at longer times^{28,76,77}. We find qualitatively the same behavior for entanglement, except that we consider a soft-UV cutoff obtaining only a partial noise suppression. Notice that at $\bar{t} = 0.1\mu\text{s}$ a concurrence larger than C_{th} is recovered with only $n = 2$ pulses by both CP and UDD sequences. They yield $C \sim 0.8$, the corresponding PDD yielding slightly worse results, being a two-pulse echo with not so large $\Delta t = 0.5/\gamma_M$. The advantage of using the CP sequence emerges at longer times. At $0.3\mu\text{s}$ entanglement is kept above the nonlocality threshold C_{th}

n	$\bar{t}_1 = 0.1\mu\text{s}$	$\bar{t}_2 = 0.3\mu\text{s}$
2	(0.905, 0.99451)	(0.049, 0.84100)
4	(0.975, 0.99945)	(0.506, 0.93661)
6	(0.989, 0.99988)	(0.734, 0.97428)
8	(0.994, 0.99996)	(0.843, 0.98796)
10	(0.996, 0.99998)	(0.896, 0.99370)

TABLE II: Values of CP sequence efficiency $\mathcal{E}_n(t)$ and fidelity $\mathcal{F}_n(t)$, displayed as $(\mathcal{E}, \mathcal{F})$, at the indicated times and different number of pulses n , for initial EWL states with $r = r_{\text{exp}} = 0.91$ and $|a| = 1/\sqrt{2}$ and $1/f$ noise figures discussed in the text.

with only 4 pulses, Fig. 8 (bottom panel). For this protocol the interval between pulses, $\Delta t_1 = \Delta t_4 = 37.5\text{ ns}$ and $\Delta t_2 = \Delta t_3 = 75\text{ ns}$, are well within current experimental resources. On the contrary PDD with $n = 4$, with $\Delta t = 4/(3\gamma_M)$, has a worse performance since the effect of fluctuators switching at $\gamma \sim \gamma_M$ is not cancelled. Notice finally that for the parameter we consider strongly coupled fluctuators, such that $\gamma \ll \bar{v} = 0.4\pi\text{MHz}$, are effectively averaged out since we consider higher pulse rates, $1/\Delta t \gg \bar{v}$ ²¹.

It should be noted that for noises with strong low-frequency component, like $1/f$ noise, there is a strong inhomogeneous broadening effect which is efficiently removed by echo and by CP sequence, in the multi-pulse case. As visible in the results shown, PDD indeed shows up as an inconvenient sequence compared to a CP sequence with the same number of pulses.

DD sequence efficiency.— The performance of each DD sequence in preserving entanglement until time t can be quantified by evaluating the efficiency defined as

$$\mathcal{E}_n(t) = C_n^{\text{DD}}(t)/C(0), \quad (15)$$

where $C_n^{\text{DD}}(t)$ is the concurrence for a given DD sequence with n pulses at time t . Another figure of merit is the fidelity to the initial EWL state given by⁷⁸

$$\mathcal{F}_n(t) = \text{Tr} \sqrt{\sqrt{\rho_i} \rho_n^{\text{DD}}(t) \sqrt{\rho_i}}, \quad (16)$$

where ρ_i is the initial EWL Eq. (2), while $\rho_n^{\text{DD}}(t)$ is the evolved state under DD control.

We list in table II the values of efficiency $\mathcal{E}_n(t)$ and fidelity $\mathcal{F}_n(t)$ for the CP sequence in the presence of $1/f$ noise at times $\bar{t}_1 = 0.1\mu\text{s}$, $\bar{t}_2 = 0.3\mu\text{s}$ and different n . We observe that the CP sequence can be very effective in protecting entanglement against $1/f$ noise up to times of the order of the total typical duration of two-qubit gate sequences⁵⁹. Moreover these results provide evidence that the CP sequence is the most effective, the entanglement being kept over the threshold C_{th} of Bell inequality violation up to times allowing for instance, for secure quantum cryptography.

VI. CONCLUSIONS

In this paper we investigated DD techniques protecting entanglement and nonlocality in a system of two noninteracting qubits subject to strong low-frequency noise, with $1/f$ spectrum. We focused on a realistic setup of distributed quantum memory, operating DD by different sequences (PDD, CP, UDD) of pulses. We used typical noise and control figures from superconducting qubits where these sequences have been recently used to mitigate single-qubit dephasing due to low-frequency noise^{35,42}. Differently from other proposals, where DD of entanglement between two qubits is realized by nonlocal control³⁸ or nested^{39,40} sequences, here we considered simple DD pulse sequences acting locally on each qubit.

In particular we focused on the question whether it is possible to preserve non-locality for a class of mixed states, allowing for applications to Quantum Technologies. To this end, first of all, we demonstrated a closed relation - Eq. (5) - between an entanglement quantifier (concurrence) and nonlocality, quantified by the Bell function. This dynamical connection among different quantum correlation quantifiers, which is the main mathematical result of our work, is valid during the system evolution under any local pure-dephasing qubit-environment interaction of systems prepared in EWL states. It implies that a threshold value of concurrence C_{th} exists, which depends on the purity of the initial state, above which the two-qubit system exhibits non-local correlations with certainty, providing a benchmark for the performance of strategies of entanglement protection. Entanglement can be preserved by local pulses since the two qubits are independent and affected by local pure dephasing noise, an effect recently pointed out in Refs⁷⁹⁻⁸¹.

We first studied pulsed control in the presence of a single RTN identifying a variety of behaviors depending on the qubit-fluctuator coupling g . We found that effects of two-pulse echo depend on whether g is smaller or larger than a threshold value \bar{g} , marking the existence of entanglement revivals in the absence of pulses. When $g \leq \bar{g}$ the ESD time is delayed, whereas when $g > \bar{g}$ the dynamical features of revivals and dark periods are canceled out by the echoes, entanglement exhibiting plateau-like behaviors. Multi pulse sequences turn out to be more efficient in entanglement preservation, prolonging the ESD time and allowing to keep $C > C_{th}$.

We then studied entanglement DD from $1/f$ noise with amplitude typically observed in superconducting nanocircuits. We have shown that entanglement and its nonlocal features can be stored very efficiently up to times an order of magnitude longer than natural entanglement disappearance times, which is the physical message of our work. These storage times are long enough to perform two-qubit quantum operations with pulse timings of current experimental reach^{35,42}.

In this manuscript we considered hard-pulses, i.e. ideal instantaneous pulses. The real finite-pulse duration could

be included in this analysis by appropriately modifying the filter functions, as in Ref.³⁵ where authors assumed square pulses (about 7 ns duration). We do not expect that this analysis would give substantial modification of our results, also in consideration of the fact that we concentrated on rather small number of pulses²⁸. Instead, we expect that numerical optimization of control pulses^{22,82,83} and realistic bounded amplitude control⁸⁴ may further improve the efficiency of the investigated entanglement memory element. Room for improvement is also expected since, as we find in our simulations for both RTN and pure dephasing $1/f$ noise, and as observed in experiments in the latter case, the CP sequence outperforms PDD and UDD. Finally, it would be interesting to extend our work to study decoupling from correlated low-frequency noise sources acting on both qubits, which produce distinctive decoherence effects in realistic solid-state quantum hardware⁸⁵.

Acknowledgments

R.L.F. and A.D. acknowledge support from the Centro Siciliano di Fisica Nucleare e Struttura della Materia (Catania). R.L.F. acknowledges support from the Brazilian funding agency CAPES [Pesquisador Visitante Especial-Grant No. 108/2012]. R.L.F. also acknowledges discussions with P. Caldara. This work is partially supported by MIUR through Grant No. PON02-00355-3391233, Tecnologie per l'ENERGIA e l'Efficienza energetica - ENERGETIC.

Appendix A: Qubit coherence in the presence of RTN and under PDD

In this appendix we report the analytic form of the single-qubit coherence in the presence of pure dephasing random telegraph noise under PDD with an even number of pulses $q_{PDD}(t)$ derived in Falci et al.²¹, D'Arrigo et al.⁷⁰. Here we put $\alpha = \sqrt{1 - g^2}$ and remind that pulses are applied at times $t = n\Delta t$

$$q_{PDD}(t) = \frac{E^{\frac{n}{2}} e^{-\frac{\gamma t}{2}}}{|\alpha|^n} \left\{ \frac{I_-}{EG_2} [E_1 + \delta p_0(E_3 + iE_2)] + I_+ \right\}, \quad (A1)$$

where

$$\begin{aligned}
E_0 &= |\alpha|^2 \left| \cosh \left(\frac{\alpha \gamma t}{2n} \right) \right|^2 + (1 + g^2) \left| \sinh \left(\frac{\alpha \gamma t}{2n} \right) \right|^2, \\
E_1 &= 2\Re \left\{ \alpha \cosh \left(\frac{\alpha \gamma t}{2n} \right) \sinh \left(\frac{\alpha \gamma t}{2n} \right)^* \right\}, \\
E_2 &= -2g \left| \sinh \left(\frac{\alpha \gamma t}{2n} \right) \right|^2, \\
E_3 &= -2g\Im \left\{ \alpha \cosh \left(\frac{\alpha \gamma t}{2n} \right) \sinh \left(\frac{\alpha \gamma t}{2n} \right)^* \right\}, \\
E &= \left[|E_0|^2 - \sum_{i=1}^3 |E_i|^2 \right]^{1/2}, \\
G_1 &= \frac{E_0}{E}, \quad G_2 = \frac{\left[\sum_{i=1}^3 |E_i|^2 \right]^{1/2}}{E}, \\
I_{\pm} &= [(G_1 + G_2)^{n/2} \pm (G_1 - G_2)^{n/2}] / 2.
\end{aligned}$$

The symbols \Re and \Im indicate, respectively, the real part and the imaginary part of the complex number.

-
- * Electronic address: rosario.lofranco@unipa.it
- ¹ W. H. Zurek, Rev. Mod. Phys. **75**, 715 (2003).
 - ² T. Yu and J. H. Eberly, Science **323**, 598 (2009).
 - ³ E. Paladino, Y. Galperin, G. Falci, and B. Altshuler, Rev. Mod. Phys. **86**, 361 (2014).
 - ⁴ Z.-L. Xiang, S. Ashhab, J. You, and F. Nori, Rev. Mod. Phys. **85**, 623 (2013).
 - ⁵ T. D. Ladd, F. Jelezko, R. Laflamme, Y. Nakamura, C. Monroe, and J. L. O'Brien, Nature **464**, 45 (2010).
 - ⁶ A. Acín, N. Gisin, and L. Masanes, Phys. Rev. Lett. **97**, 120405 (2006).
 - ⁷ N. Gisin and R. Thew, Nature Photon. **1**, 165 (2007).
 - ⁸ S. Pironio, A. Acín, S. Massar, A. B. de la Giroday, D. N. Matsukevich, P. Maunz, S. Olmschenk, D. Hayes, L. Luo, T. A. Manning, and C. Monroe, Nature **464**, 1021 (2010).
 - ⁹ M. Lucamarini, G. Vallone, I. Gianani, G. D. Giuseppe, and P. Mataloni, Phys. Rev. A **86**, 032325 (2012).
 - ¹⁰ R. Horodecki, P. Horodecki, M. Horodecki, and K. Horodecki, Rev. Mod. Phys. **81**, 865 (2009).
 - ¹¹ B. Bellomo, R. Lo Franco, and G. Compagno, Phys. Rev. A **78**, 062309 (2008).
 - ¹² L. Viola and S. Lloyd, Phys. Rev. A **58**, 2733 (1998).
 - ¹³ L. M. K. Vandersypen and I. L. Chuang, Rev. Mod. Phys. **76**, 1037 (2005).
 - ¹⁴ H. M. Wiseman and G. J. Milburn, *Quantum Measurement and Control* (Cambridge University Press, USA, New York, 2010).
 - ¹⁵ W. B. Mims, *Electron Paramagnetic Resonance* (New York: Plenum, 1972), pp. 263–351.
 - ¹⁶ L. Viola, E. Knill, and S. Lloyd, Phys. Rev. Lett. **82**, 2417 (1999).
 - ¹⁷ H. Y. Carr and E. M. Purcell, Phys. Rev. **94**, 630 (1954).
 - ¹⁸ G. S. Uhrig, Phys. Rev. Lett. **98**, 100504 (2007).
 - ¹⁹ W. Yang and R.-B. Liu, Phys. Rev. Lett. **101**, 180403 (2008).
 - ²⁰ M. J. Biercuk, A. C. Doherty, and H. Uys, J. Phys. B: At. Mol. Opt. Phys. **44**, 154002 (2011).
 - ²¹ G. Falci, A. D'Arrigo, A. Mastellone, and E. Paladino, Phys. Rev. A **70**, 040101(R) (2004).
 - ²² P. Rebentrost, I. Serban, T. Schulte-Herbruggen, and F. K. Wilhelm, Phys. Rev. Lett. **102**, 090401 (2009).
 - ²³ R. M. Lutchyn, L. Cywiński, C. P. Nave, and S. Das Sarma, Phys. Rev. B **78**, 024508 (2008).
 - ²⁴ L. Faoro and L. Viola, Phys. Rev. Lett. **92**, 117905 (2004).
 - ²⁵ J. Bergli and L. Faoro, Phys. Rev. B **75**, 054515 (2007).
 - ²⁶ B. Cheng, Q. H. Wang, and R. Joynt, Phys. Rev. A **78**, 022313 (2008).
 - ²⁷ H. Gutmann, F. K. Wilhelm, W. M. Kaminsky, and S. Lloyd, Phys. Rev. A **71**, 020302(R) (2005).
 - ²⁸ L. Cywiński, R. M. Lutchyn, C. P. Nave, and S. Das Sarma, Phys. Rev. B **77**, 174509 (2008).
 - ²⁹ J. F. Du, X. Rong, N. Zhao, Y. Wang, J. Yang, and R. B. Liu, Nature **461**, 1265 (2009).
 - ³⁰ B. Lee, W. M. Witzel, and S. Das Sarma, Phys. Rev. Lett. **100**, 160505 (2008).
 - ³¹ Y. Nakamura, Y. A. Pashkin, T. Yamamoto, and J. S. Tsai, Phys. Rev. Lett. **88**, 047901 (2002).
 - ³² P. Bertet, I. Chiorescu, G. Burkard, K. Semba, C. J. P. M. Harmans, D. DiVincenzo, and J. E. Mooij, Phys. Rev. Lett. **95**, 257002 (2005).
 - ³³ G. Ithier, E. Collin, P. Joyez, P. J. Meeson, D. Vion, D. Esteve, F. Chiarello, A. Shnirman, Y. Makhlin, J. Schrief, and G. Schön, Phys. Rev. B **72**, 134519 (2005).
 - ³⁴ F. Yoshihara, K. Harrabi, A. O. Niskanen, Y. Nakamura, and J. S. Tsai, Phys. Rev. Lett. **97**, 167001 (2006).
 - ³⁵ J. Bylander et al., Nature Phys. **7**, 565 (2011).
 - ³⁶ F. Yan, J. Bylander, S. Gustavsson, F. Yoshihara, K. Harrabi, D. G. Cory, T. P. Orlando, Y. Nakamura, J.-S. Tsai, and W. D. Oliver, Phys. Rev. B **85**, 174521 (2012).
 - ³⁷ T. Yuge, S. Sasaki, and Y. Hirayama, Phys. Rev. Lett. **107**, 170504 (2011).
 - ³⁸ M. Mukhtar, T. B. Saw, W. T. Soh, and J. Gong, Phys. Rev. A **81**, 012331 (2010).
 - ³⁹ M. Mukhtar, W. T. Soh, T. B. Saw, and J. Gong, Phys. Rev. A **82**, 052338 (2010).
 - ⁴⁰ Z.-Y. Wang and R.-B. Liu, Phys. Rev. A **83**, 022306 (2011).

- (2011).
- ⁴¹ Y. Pand, Z.-R.-Xi, and J. Gong, J. Phys. B: At. Mol. Opt. Phys. **44**, 175501 (2011).
 - ⁴² S. Gustavsson, F. Yan, J. Bylander, F. Yoshihara, Y. Nakamura, T. P. Orlando, and W. D. Oliver, Phys. Rev. Lett. **109**, 010502 (2012).
 - ⁴³ Y. Wang, X. Rong, P. Feng, W. Xu, B. Chong, J.-H. Su, J. Gong, and J. Du, Phys. Rev. Lett. **106**, 040501 (2011).
 - ⁴⁴ S. S. Roy, T. S. Mahesh, and G. S. Agarwal, Phys. Rev. A **83**, 062326 (2011).
 - ⁴⁵ M. D. Shulman, O. E. Dial, S. P. Harvey, H. Bluhm, V. Umansky, and A. Yacoby, Science **336**, 202 (2012).
 - ⁴⁶ F. Dolde, I. Jakobi, B. Naydenov, N. Zhao, S. Pezzagna, C. Trautmann, J. Meijer, P. Neumann, F. Jelezko, and J. Wrachtrup, Nature Phys. **9**, 139 (2013).
 - ⁴⁷ W. K. Wootters, Phys. Rev. Lett. **80**, 2245 (1998).
 - ⁴⁸ M. Horodecki, P. Horodecki, and R. Horodecki, Phys. Lett. A **200**, 340 (1995).
 - ⁴⁹ L. Mazzola, B. Bellomo, R. Lo Franco, and G. Compagno, Phys. Rev. A **81**, 052116 (2010).
 - ⁵⁰ B. Horst, K. Bartkiewicz, and A. Miranowicz, Phys. Rev. A **87**, 042108 (2013).
 - ⁵¹ K. Bartkiewicz, B. Horst, K. Lemr, and A. Miranowicz, Phys. Rev. A **88**, 052105 (2013).
 - ⁵² F. Verstraete and M. M. Wolf, Phys. Rev. Lett. **89**, 170401 (2002).
 - ⁵³ B. Bellomo, R. Lo Franco, and G. Compagno, Phys. Rev. Lett. **99**, 160502 (2007).
 - ⁵⁴ T. Yu and J. H. Eberly, Quantum Information and Computation **7**, 459 (2007).
 - ⁵⁵ B. Bellomo, R. Lo Franco, and G. Compagno, Phys. Lett. A **374**, 3007 (2010).
 - ⁵⁶ A. Miranowicz, Phys. Lett. A **327**, 272 (2004).
 - ⁵⁷ B. Bellomo, R. Lo Franco, and G. Compagno, Adv. Science Lett. **2**, 459 (2009).
 - ⁵⁸ N. Gisin, Phys. Lett. A **154**, 201 (1991).
 - ⁵⁹ L. DiCarlo, J. M. Chow, J. M. Gambetta, L. S. Bishop, B. R. Johnson, D. I. Schuster, J. Majer, A. Blais, L. Frunzio, S. M. Girvin, and R. J. Schoelkopf, Nature **460**, 240 (2009).
 - ⁶⁰ L. D. Carlo, M. D. Reed, L. Sun, B. R. Johnson, J. M. Chow, J. M. Gambetta, L. Frunzio, S. M. Girvin, M. H. Devoret, and R. J. Schoelkopf, Nature **467**, 574 (2010).
 - ⁶¹ M. Neeley, R. C. Bialczak, M. Lenander, E. Lucero, M. Mariantoni, A. D. O'Connell, D. Sank, H. Wang, M. Weides, J. Wenner, Y. Yin, T. Yamamoto, A. N. Cleland, and J. M. Martinis, Nature **467**, 570 (2010).
 - ⁶² E. Lucero, R. Barends, Y. Chen, J. Kelly, M. Mariantoni, A. Megrant, P. O'Malley, D. Sank, A. Vainsencher, J. Wenner, T. White, Y. Yin, A. N. Cleland, and J. M. Martinis, Nat. Phys. **8**, 719 (2012).
 - ⁶³ M. Mariantoni, H. Wang, T. Yamamoto, M. Neeley, R. C. Bialczak, Y. Chen, M. Lenander, E. Lucero, A. D. O'Connell, D. Sank, M. Weides, J. Wenner, Y. Yin, J. Zhao, A. N. Korotkov, A. N. Cleland, and J. M. Martinis, Science **334**, 61 (2011).
 - ⁶⁴ A. Fedorov, L. Steffen, M. Baur, M. P. da Silva, and A. Wallraff, Nature **481**, 170 (2012).
 - ⁶⁵ M. D. Reed, L. DiCarlo, S. E. Nigg, L. Sun, L. Frunzio, S. M. Girvin, and R. J. Schoelkopf, Nature **482**, 382 (2012).
 - ⁶⁶ J. M. Chow, J. M. Gambetta, A. D. Corcoles, S. T. Merkel, J. A. Smolin, C. Rigetti, S. Poletto, G. A. Keefe, M. B. Rothwell, J. R. Rozen, M. B. Ketchen, and M. Steffen, Phys. Rev. Lett. **109**, 060501 (2012).
 - ⁶⁷ C. Rigetti, J. M. Gambetta, S. Poletto, B. L. T. Plourde, J. M. Chow, A. D. Corcoles, J. A. Smolin, S. T. Merkel, J. R. Rozen, G. A. Keefe, M. B. Rothwell, M. B. Ketchen, and M. Steffen, Phys. Rev. B **86**, 100506(R) (2012).
 - ⁶⁸ M. B. Weissman, Rev. Mod. Phys. **60**, 537 (1988).
 - ⁶⁹ E. Paladino, L. Faoro, G. Falci, and R. Fazio, Phys. Rev. Lett. **88**, 228304 (2002).
 - ⁷⁰ A. D'Arrigo, G. Flaci, A. Mastellone, and E. Paladino, Physica E **29**, 297 (2005).
 - ⁷¹ D. Zhou, A. Lang, and R. Joynt, Quantum Inf. Process. **9**, 727 (2010).
 - ⁷² R. Lo Franco, A. D'Arrigo, G. Falci, G. Compagno, and E. Paladino, Phys. Scripta **T147**, 014019 (2012).
 - ⁷³ Y. M. Galperin, B. L. Altshuler, J. Bergli, and D. V. Shantsev, Phys. Rev. Lett. **96**, 097009 (2006).
 - ⁷⁴ G. Falci, A. D'Arrigo, A. Mastellone, and E. Paladino, Phys. Rev. Lett. **94**, 167002 (2005).
 - ⁷⁵ B. Bellomo, G. Compagno, A. D'Arrigo, G. Falci, R. Lo Franco, and E. Paladino, Phys. Rev. A **81**, 062309 (2010).
 - ⁷⁶ S. Pasini and G. S. Uhrig, Phys. Rev. A **81**, 012309 (2010).
 - ⁷⁷ Z.-Y. Wang and R.-B. Liu, Phys. Rev. A **87**, 042319 (2013).
 - ⁷⁸ M. A. Nielsen and I. L. Chuang, *Quantum Computation and Quantum Information* (Cambridge, UK, Cambridge University Press, 2000).
 - ⁷⁹ A. D'Arrigo, R. Lo Franco, G. Benenti, E. Paladino, and G. Falci, arXiv:1207.3294.
 - ⁸⁰ A. D'Arrigo, R. Lo Franco, G. Benenti, E. Paladino, and G. Falci, Phys. Scripta **T153**, 014014 (2013).
 - ⁸¹ A. D'Arrigo, G. Benenti, R. Lo Franco, G. Falci, and E. Paladino, Int. J. Quant. Inf. **12**, 1461005 (2014).
 - ⁸² M. Möttönen, R. de Sousa, J. Zhang, and K. B. Whaley, Phys. Rev. A **73**, 022332 (2006).
 - ⁸³ G. Gordon, G. Kurizki, and D. A. Lidar, Phys. Rev. Lett. **101**, 010403 (2008).
 - ⁸⁴ D. J. Gorman, K. C. Young, and K. B. Whaley, Phys. Rev. A **86**, 012317 (2012).
 - ⁸⁵ A. D'Arrigo, G. Falci, A. Mastellone, and E. Paladino, New J. Phys. **10**, 115006 (2008).